Supercurrent in Atomic Point Contacts and Andreev States

M. F. Goffman,[1] R. Cron,[1] A. Levy Yeyati,[2] P. Joyez,[1] M. H. Devoret,[1] D. Esteve,[1] and C. Urbina[1]

[1]*Service de Physique de l'Etat Condensé, CEA-Saclay, F-91191 Gif-sur-Yvette Cedex, France*

[2]*Departamento de Física Teórica de la Materia Condensada C-V, Universidad Autónoma de Madrid, E-28049 Madrid, Spain*

(Received 13 December 1999)

We have measured the supercurrent in aluminum atomic point contacts containing a small number of well characterized conduction channels. For most contacts, the measured supercurrent is adequately described by the opposite contributions of two thermally populated Andreev bound states per conduction channel. However, for contacts containing an almost perfectly transmitted channel $0.9 \leq \tau \leq 1$ the measured supercurrent is higher than expected, a fact that we attribute to nonadiabatic transitions between bound states.

PACS numbers: 73.40.Jn, 73.20.Dx, 74.50.+r

In 1962, Josephson predicted that a surprisingly large supercurrent could flow between two weakly coupled superconducting electrodes when a phase difference δ is applied across the whole structure. This phase-driven supercurrent $I(\delta)$ has subsequently been observed in a variety of weak coupling configurations such as thin insulating barriers, narrow diffusive wires, and ballistic point contacts between large electrodes. However, a theoretical framework powerful enough to predict the current-phase relation $I(\delta)$ in all configurations has emerged only during the last decade [1]. It applies in the mesoscopic regime, when electron transport between the electrodes is a quantum coherent process. Such transport is described by a set of N transmission coefficients $\{\tau_i\}$ corresponding to N independent conduction channels. In the normal state, the conductance is given by $G_0 \sum_{i=1}^{N} \tau_i$ where $G_0 = 2e^2/h$ is the conductance quantum. In the superconducting state, electrons (holes) transmitted in one channel are Andreev reflected at the electrodes into holes (electrons) in the same channel. After a cycle involving two reflections at the electrodes, they acquire at the Fermi energy an overall phase factor $\pi + \delta$ (Fig. 1). In a "short" coupling structure, these cycles give rise to two electron-hole resonances per channel, called Andreev bound states (AS) [2] with energies $E_{\pm}(\delta, \tau_i) = \pm\Delta[1 - \tau_i \sin^2(\delta/2)]^{1/2}$ (Δ is the energy gap in the electrodes). These two AS carry current in opposite directions, $I_{\pm}(\delta, \tau) = \varphi_0^{-1}\, dE_{\pm}(\delta, \tau_i)/d\delta$ (where $\varphi_0 = \hbar/2e$), and the net supercurrent results from the imbalance of their populations. A quantitative comparison of the predictions of this "mesoscopic superconductivity" picture of the Josephson effect with experimental results is usually hindered by the fact that in most devices the current flows through a very large number of channels with unknown τ_i. However, an atomic-size constriction between two electrodes, referred to hereafter simply as an atomic contact [3], is an extreme type of weak coupling structure which accommodates just a few channels. Because their set $\{\tau_i\}$ is amenable to a complete experimental determination and because it can be controlled in a certain range [4], atomic contacts are ideal systems on which to test quantitatively the concepts of mesoscopic physics. The knowledge of $\{\tau_i\}$ allows in principle the calculation of all transport quantities. In particular, the phase-driven supercurrent is given by

$$I_J(\delta, \{\tau_i\}, \{n_{i\pm}\}) = \sum_{i=1}^{N} (n_{i-} - n_{i+}) I_-(\delta, \tau_i), \quad (1)$$

where $n_{i\pm}$ are the occupation numbers of the two AS associated with the ith channel. The critical current of the contact is the maximum of this current-phase relationship at zero temperature $I_0(\{\tau_i\}) = \max_{\delta}[I_J(\delta, \{\tau_i\}, n_{i+} = 0, n_{i-} = 1)]$. In this Letter, we present an

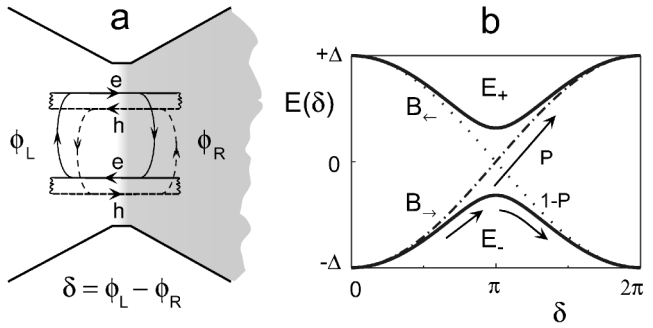

FIG. 1. (a) Josephson coupling through a single channel of transmission τ between two superconducting electrodes with phase difference $\delta = \phi_L - \phi_R$. Wavy lines represent Andreev scattering mechanism: electrons (holes) are reflected as holes (electrons) at the electrodes. Upward and downward arrows represent normal scattering, which couples electron (hole) states with backward electron (hole) states. (b) Combination of both scattering mechanisms results in two "Andreev bound states" with phase dependent energies $E_{\pm}$ (full lines). Gap at $\delta = \pi$ is $2\Delta\sqrt{1 - \tau}$. P is interlevel nonadiabatic transition probability at $\delta = \pi$. Dash-dotted (dotted) line is $B_{\rightarrow}(B_{\leftarrow})$ ballistic state for $\tau = 1$, carrying current towards the right (left).

 0031-9007/00/85(1)/170(4)$15.00

experiment on aluminum atomic contacts in which we compare the measured supercurrent with the predictions of this mesoscopic Josephson effect theory.

In practice the measurement of a supercurrent is not done by imposing a phase difference across the device [5] but by biasing it with a dc current and detecting the maximum current at zero voltage. As the Josephson coupling introduced between the two electrodes by a single channel of transmission τ has a small characteristic energy $E_J = \varphi_0 I_0(\tau) \leq \varphi_0 I_0(\tau = 1) = \Delta/2$ (for Al, $E_J \leq 1 k_B K$), the phase difference δ is prone to both quantum and thermal fluctuations, which depend not only on the parameters of the contact but also on the circuit in which the contact is embedded. In fact, unless this electromagnetic environment is carefully designed so as to damp phase fluctuations [6], the supercurrent time averages to nearly zero and the observed maximum supercurrent is much smaller than I_0 [3]. We have thus integrated microfabricated mechanically controllable break junctions [7] into an adequate on-chip dissipative environment (see Fig. 2). Current-voltage characteristics (IV) were measured using a four-probe geometry. Each line contains a small resistor close to the atomic contact, and also a large capacitor to the underlying ground plane formed by the substrate. The equivalent circuit of the setup is shown in the right inset of Fig. 2. The atomic contact is characterized by (1) and its capacitance C_J. It is connected through a resistor R to a current source I_b in parallel with a capacitance C. We now concentrate on one-atom aluminum contacts which typically accommodate three channels and have a conductance of order G_0 [4]. A typical IV measured at the lowest temperature is shown in Fig. 3. The strong nonlinearities in the finite voltage (dissipative) branch are associated [8] with multiple Andreev reflection processes and allow the determination of $\{\tau_i\}$ [4]. The supercurrent branch appears on large voltage scales as a vertical line at $V \sim 0$. However, the upper inset of Fig. 3 shows that for finite current there is always a finite voltage across the contact. When the bias current is ramped repeatedly, the system switches to the dissipative branch at a value I_s which fluctuates from cycle to cycle. The slope of the supercurrent branch and the average switching current $\langle I_s \rangle$ both decrease when increasing the temperature.

Given the simplicity of the biasing circuit, the exact shape of the supercurrent branch can be calculated. Following the analysis of [6] the circuit is described by two dynamical variables, δ and u (the ratio between the voltage across the capacitor C and RI_0), and three environment parameters: a characteristic time $t_J = \varphi_0/RI_0$ and the damping factors $\alpha_0 = \varphi_0/R^2 I_0 C_J$ and $\alpha = R^2 C I_0/\varphi_0$. For all the measured contacts the environment parameters were chosen such that $\alpha_0 \gg 1$ [9], and the current through C_J can thus be neglected. In this classical regime, the time evolution of the circuit is governed by two dimensionless equations,

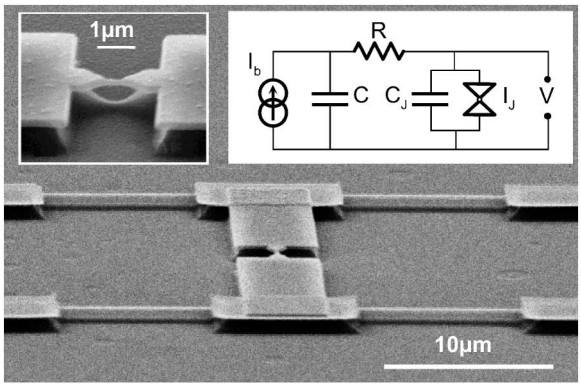

FIG. 2. Micrograph of Al microbridge in a dissipative environment. Each IV probe contains a AuCu (weight ratio 3:1) resistor (10 μm-long, 500 nm wide, and 30 or 50 nm thick) and a large (2.5 mm)^2, 180 nm thick AuCu/Al pad (not shown) that forms with the metallic substrate a large capacitor. Substrate is phosphor-bronze covered by a 2 μm thick layer of polyimide. Left inset: side view of bridge (150 nm thick Al layer with 100 nm wide constriction in the middle) suspended by selective etching of polyimide. Bridge is broken by controlled bending of the substrate at low temperatures ($T < 1$ K) and under cryogenic vacuum to prevent contamination of the two resulting electrodes. Right inset: equivalent circuit. The atomic contact (double triangle symbol) is connected to a current source through a resistor R. The capacitors on each line combine into the capacitor C. Total capacitance between the two sides of the bridge is C_J. The voltage V across the contact is related to the phase velocity through the Josephson relation $\varphi_0 \dot{\delta} = V$.

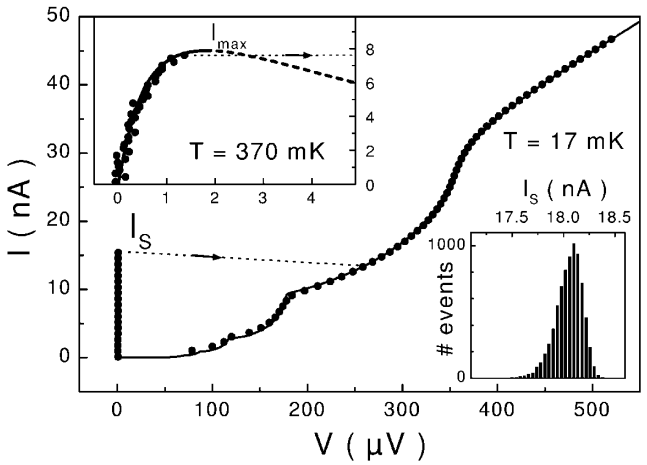

FIG. 3. Large scale IV characteristic of atomic contact, measured at 17 mK (dots). Switching at current I_s from supercurrent branch (almost vertical branch near zero voltage) to dissipative branch is a stochastic process. Full line is the best fit of this branch, obtained by decomposing the total current into contributions of 3 independent channels, giving $\{\tau_i\} = \{0.52, 0.26, 0.26\}$ and $I_0 = 25.3 \pm 0.4$ nA. Top inset: expanded view of experimental (dots) and theoretical (lines) diffusion branch at 370 mK (thick dashed line shows negative differential resistance region). Bottom inset: I_s histogram measured at $T = 17$ mK and $dI/I_0\, dt = 581\ \mathrm{s}^{-1}$.

$$\frac{d\delta}{dt} = u - i_J(\delta) + i_n(t), \tag{2}$$

$$\alpha \frac{du}{dt} = i_b - i_J(\delta). \tag{3}$$

Here, time is in units of t_J, $i_J(\delta) = I_J(\delta)/I_0$, and $i_b = I_b/I_0$. The thermal current noise source $i_n(t)$ associated with the resistor obeys the fluctuation-dissipation theorem. If R and C are large enough to achieve $\alpha \gg 1$ (keeping, however, $R \ll h/4e^2$ to avoid quantum fluctuations of δ [10]), the time evolution of u is much slower than that of δ. One then first solves (2) with a constant u and afterwards solves (3) for the slower dynamics of u. The first step is equivalent to solving the resistively shunted junction model [11] with a voltage source u. As in the well-known case of tunnel junctions, the dynamics of the phase in this circuit is equivalent to the Brownian motion of a massless particle in a tilted washboardlike "potential," governed by the Langevin equation (2). However, here the potential is not the usual tilted sinusoid but has instead the more general form [12]

$$U_p = -u\delta + \sum_{i=1}^{N} (n_{i+} - n_{i-}) E_-(\delta, \tau_i), \tag{4}$$

which depends on $\{\tau_i\}$ and the time dependent $n_{i\pm}$. Several mechanisms can make these $n_{i\pm}$ change, but in general none is very efficient. The relaxation induced by phonons has been addressed in [13]. We have found that the relaxation of the upper state through the emission of photons in the environment is extremely slow except for highly transmitted channels at $\delta \sim \pi$ [14]. However, relaxation by the exchange of quasiparticles with states in the bulk electrodes can be very fast, but only at $\delta = 0$ (Fig. 1). We have solved (2) by making a straightforward generalization of the procedure introduced by Ambegaokar and Halperin [15] for overdamped tunnel junctions. In this adiabatic model the "particle" moves in a constant potential obtained by replacing in (4) the $n_{i\pm}$ by their thermal equilibrium values at $\delta = 0$ [16].

The upper inset of Fig. 3 shows a comparison of the measured supercurrent branch for a particular contact with the predictions of this adiabatic model. The supercurrent branch is, in fact, a current peak. The equivalent particle is constantly thermally activated over the potential barriers between the wells and undergoes a classical diffusion motion with a small, friction-limited drift velocity. The only inputs of the calculation are the temperature, R, and the measured values of $\{\tau_i\}$, which determine the zero temperature supercurrent I_0 [17]. The value of R, which is measured independently, sets only the voltage scale of the supercurrent peak. In our RC biasing scheme, which keeps the atomic contact unshunted at dc, the negative differential resistance region of the IV is unstable, and the system switches to the dissipative branch before reaching the maximum $I_{\max}$ of the current peak. The capacitor was designed large enough ($C = 140$ pF) for all the samples to be in the overdamped limit $\alpha \gg 1$, in which case I_s is predicted to be close to $I_{\max}$. The fluctuations of I_s are also small, as shown by the narrow switching current histogram in the bottom inset of Fig. 3.

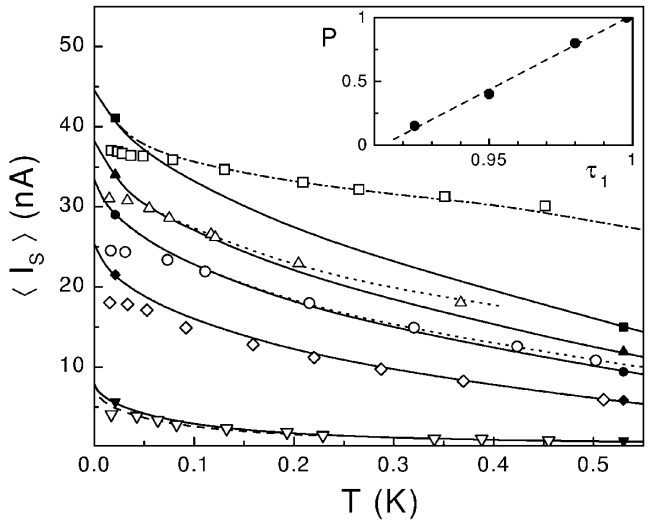

FIG. 4. Experimental (open symbols) and theoretical (lines) average switching current $\langle I_s \rangle$ as a function of temperature for different contacts on two samples. ($\triangledown$) $\{\tau_i\} = \{0.21, 0.07, 0.07\}$, $I_0 = 8.0 \pm 0.1$ nA [17]. ($\diamond$) $\{\tau_i\} = \{0.52, 0.26, 0.26\}$, $I_0 = 25.3 \pm 0.4$ nA. ($\circ$) $\{\tau_i\} = \{0.925, 0.02, 0.02\}$, $I_0 = 33.4 \pm 0.4$ nA. ($\triangle$) $\{\tau_i\} = \{0.95, 0.09, 0.09, 0.09\}$, $I_0 = 38.8 \pm 0.2$ nA. ($\square$) $\{\tau_i\} = \{0.998, 0.09, 0.09, 0.09\}$, $I_0 = 44.2 \pm 0.9$ nA. Contacts ($\triangledown$), ($\diamond$), ($\triangle$), and ($\square$) from sample with $\Delta/e = 178 \pm 1$ μV, $R = 125 \pm 10$ Ω. Contact ($\circ$) from sample with $\Delta/e = 184.5 \pm 1.0$ μV, $R = 170 \pm 20$ Ω. Full lines (with solid symbols): predictions of adiabatic theory for $\alpha \to \infty$, for which $\langle I_s \rangle \to I_{\max}$. Dashed line: finite α corrections for contact ($\triangledown$). Dash-dotted line: predictions of adiabatic theory for contact ($\square$), assuming the highest transmitted channel to be ballistic. Dotted lines: predictions of extended model including empirical interlevel nonadiabatic transition probability P at $\delta = \pi$ ($P = 0.4$ for upper curve, $P = 0.15$ for lower one). Inset: probability P as a function of transmission coefficient τ_1 of highest transmitted channel for different contacts displaying extra supercurrent. Symbols are best fits values from simulation. Dotted line is guide for the eye.

The temperature dependence of $\langle I_s \rangle$ measured for five contacts is shown in Fig. 4 together with the predictions of the adiabatic model sketched above. For every contact having all channels such that $\tau_i \lesssim 0.9$ the $\alpha \to \infty$ limit of the theory describes well the data at high temperature. Moreover, in the case of very low τ, finite α corrections can be calculated [6] and explain the small deviations at intermediate temperatures. We attribute the remaining low temperature deviations to the saturation of the electronic temperature in the resistors [18]. The uppermost data points in Fig. 4 correspond to a contact in which one of the channels had $\tau = 0.998$. The measured $\langle I_s \rangle$ are larger than predicted by the adiabatic theory for this τ. However, if we assume this channel to be perfectly transmitted ($\tau = 1$), a reasonable assumption given our accuracy in the determination of the τ's, we recover a very satisfactory fit

of the data. This is due to the fact that this small change in τ has a profound impact on the shape of the potential. For $\tau = 1$ the AS singularly become the ballistic $B_{\rightleftarrows}$ states (Fig. 1), which have no extrema at $\delta = \pi$. In this case the current flows always in the same direction, thus leading to a much larger average value. For contacts having at least one channel with $\tau_i \geq 0.9$, but definitely not ballistic within the experimental accuracy, the measured $\langle I_s \rangle$ is also larger than the predictions of the adiabatic theory, which corresponds in principle to the maximum observable $\langle I_s \rangle$. A possible explanation of this excess supercurrent could be the existence of transitions between the adiabatic $E_{\pm}$ states (Fig. 1), induced by the fast dynamics of δ. In the case of an almost perfectly transmitted channel ($\tau \simeq 1$), the energy gap $2\Delta\sqrt{1 - \tau}$ at $\delta = \pi$ is very small. If the system starts a $[\delta : 0 \rightarrow 2\pi]$ cycle in the lower adiabatic state E_-, there is a finite probability P for finding it in the excited adiabatic state E_+ after δ has diffused across the region around π at finite speed (Fig. 1). For a large P the system would follow most of the time just the ballistic state $B_{\rightarrow}$, making the time-averaged supercurrent resistant to thermal fluctuations, as observed experimentally. Note that this strong nonequilibrium occupation of the AS marks the uprising of the dissipative current [19]. We have extended our model in a minimal way by adding to the boundary conditions of thermal equilibrium at $\delta = 0$, the possibility of interlevel transitions at $\delta = \pi$, with an empirical, temperature independent probability P. As shown in Fig. 4, this modified model allows fitting the experimental data reasonably well. The inset of Fig. 4 shows the best-fit value of P obtained using this procedure, as a function of the τ of the highest transmitted channel. We note that the standard Landau-Zener theory [19] predicts much too small values of P given the small drift velocity of the phase. In fact, the Landau-Zener theory is not directly applicable to the present situation in which the phase is not an external parameter swept at a constant rate, but is instead a dynamical variable undergoing a driven diffusive motion. A rigorous theory of this dissipative nonadiabatic mechanism, valid for arbitrary transmission, remains to be developed for our system, along the lines of [20] or [21], for example.

In conclusion, superconducting atomic contacts can sustain supercurrents close to that predicted solely from their mesoscopic transmission set. The value of the supercurrent is thus related to the dissipative branch of the *IV* characteristics, like in usual macroscopic Josephson junctions, although in the latter the contribution of the different channels cannot be disentangled. More generally, our findings strongly support the idea of the supercurrent being carried by Andreev bound states and show that the concepts of mesoscopic superconductivity can be applied down to the level of single atom contacts.

We acknowledge the technical assistance of P. F. Orfila and discussions with D. Averin, J. C. Cuevas, M. Feigel'man, A. Martín-Rodero, Y. Naveh, H. Pothier, and A. Shytov. M. F. G. acknowledges support by FOMEC.

[1] Entry points into the literature: P. Bagwell, R. Riedel, and L. Chang, Physica (Amsterdam) **203B**, 475 (1994); V. S. Shumeiko and E. N. Bratus, J. Low Temp. Phys. **23**, 181 (1997); A. Martín-Rodero, A. Levy Yeyati, and J. C. Cuevas, Superlattices Microstruct. **25**, 927 (1999).

[2] A. Furusaki and M. Tsukada, Solid State Commun. **78**, 299 (1991); C. W. J. Beenakker and H. van Houten, Phys. Rev. Lett. **66**, 3056 (1991).

[3] J. M. van Ruitenbeek, in *Mesoscopic Electron Transport*, edited by L. L. Sohn, L. P. Kouwenhoven, and G. Schön, NATO ASI, Ser. E, Vol. 345 (Kluwer, Dordrecht, 1997).

[4] E. Scheer *et al.*, Phys. Rev. Lett. **78**, 3535 (1997); E. Scheer *et al.*, Nature (London) **394**, 154 (1998).

[5] With one remarkable exception: M. C. Koops, G. V. van Duyneveldt, and R. de Bruyn Ouboter, Phys. Rev. Lett. **77**, 2542 (1996).

[6] D. Vion *et al.*, Phys. Rev. Lett. **77**, 3435 (1996); P. Joyez *et al.*, J. Supercond. **12**, 757 (1999).

[7] J. M. van Ruitenbeek *et al.*, Rev. Sci. Instrum. **67**, 108 (1996).

[8] These nonlinearities follow the temperature and magnetic field dependence of the gap and are not related to spurious electromagnetic resonances in the external circuit. See E. Scheer *et al.*, Physica (Amsterdam) **280B**, 425 (2000).

[9] We estimate $C_J \leq 2$ fF from the measured capacitance between a metallic pad and the ground plane (28 aF/μm^2).

[10] G.-L. Ingold and H. Grabert, Phys. Rev. Lett. **83**, 3721 (1999).

[11] D. E. McCumber, J. Appl. Phys. **39**, 3113 (1968).

[12] D. V. Averin, A. Bardas, and H. T. Imam, Phys. Rev. B **58**, 11 165 (1998).

[13] D. A. Ivanov and M. V. Feigel'man, JETP Lett. **68**, 890 (1998).

[14] Values of δ are given modulo 2π throughout this paper.

[15] V. Ambegaokar and B. I. Halperin, Phys. Rev. Lett. **22**, 1364 (1969).

[16] A numerical simulation of Langevin equation (2), with $n_{i\pm}$ selected according to a thermal equilibrium probability each time δ goes through 0, gives the same results.

[17] The set $\{\tau_i\}$ is determined by probing all possible combinations with a transmission step of 10^{-3}. The uncertainty on I_0 is obtained taking into account all $\{\tau_i\}$ fitting the *IV* with an accuracy better than 1%, a conservative estimate of the actual experimental accuracy.

[18] For the power levels dissipated in the resistors we do not expect them to cool much below 100 mK. See M. Henny *et al.*, Appl. Phys. Lett **71**, 773 (1997).

[19] D. Averin and A. Bardas, Phys. Rev. Lett. **75**, 1831 (1995); Phys. Rev. B **53**, R1705 (1996).

[20] E. Shimshoni and A. Stern, Phys. Rev. B **47**, 9523 (1993).

[21] A. V. Shytov, cond-mat/0001012.